Surface & Coatings Technology 309 (2017) 6–11

Contents lists available at ScienceDirect

Surface & Coatings Technology

journal homepage: www.elsevier.com/locate/surfcoat

Electrochemically shape-controlled transformation of magnetron sputtered platinum films into platinum nanostructures enclosed by high-index facets

Ivan Khalakhan [a,*], Jaroslava Lavková [a,b], Iva Matolínová [a], Mykhailo Vorokhta [a], Valérie Potin [b], Peter Kúš [a], Michal Václavů [a], Valentin-Adrian Maraloiu [c], Andrei-Cristian Kuncser [c], Vladimír Matolín [a]

[a] Charles University, Faculty of Mathematics and Physics, Department of Surface and Plasma Science, V Holešovičkách 2, 18000 Prague 8, Czech Republic
[b] ICB - Laboratoire Interdisciplinaire Carnot de Bourgogne, UMR 6303 CNRS-Université de Bourgogne, 9 Av. A. Savary, BP 47870, F-21078 Dijon Cedex, France
[c] National Institute of Material Physics, 405A Atomistilor St., 077125, Magurele, Bucharest, Romania

ARTICLE INFO

Article history:
Received 25 July 2016
Revised 13 October 2016
Accepted in revised form 6 November 2016
Available online 09 November 2016

Keywords:
Platinum
Thin films
Transformation
Nanostructures
High-index facet
Shape dependence

ABSTRACT

A new method based on transformation of magnetron sputtered platinum thin films into platinum nanostructures enclosed by high-index facets, using electrochemical potential cycling in a twin working electrode system is reported. The controllable formation of various Pt nanostructures, described in this paper, indicates that this method can be used to control a selective growth of high purity Pt nanostructures with specific shapes (facets or edges). The method opens up new possibilities for electrochemical preparation of nanostructured Pt catalysts at high yield.

1. Introduction

Noble metal nanocrystals (NCs) have received attention from scientists over the past few years because of their broad applications in catalysis [1–3]. Ability to control NCs size, shape, crystallinity, and composition provides opportunity to tune their catalytic activity and selectivity [4–9]. The performance of nanocrystals used as catalysts depends strongly on their surface structure, particularly facets enclosing the crystals. It was shown that Pt high-index planes with open surface structure exhibit much higher reactivity in comparison to (111) or (100) close-packed low-index planes because high-index planes have a large density of atomic steps, edges, kinks, which are especially important in catalytic reactions [10,11]. Thus, the metal nanoparticles or nanostructures with high-index facets represent novel and very promising types of catalysts. However, it is challenging to synthesize shape-controlled high-index facets NCs, which are in general thermodynamically unfavorable [12].

Over the past decade, many methods have been developed to produce noble metal NCs enclosed by high-index facets in well-controlled way [13]. The most remarkable progress, however, has been made using electrochemical methods in recent years. Pt triambic icosahedral nanocrystals enclosed by {771} high-index facets, electrochemically deposited from H_2PtCl_6 solution and shape-controlled exhibited higher electrocatalytic activity and stability towards ethanol electrooxidation than a commercial Pt black catalyst [14]. Platinum dendrites enclosed by {331} facets were prepared using similar method for methanol catalytic combustion [15]. Tian et al. made a breakthrough in synthesis of Pt nanocrystals enclosed by high-index facets by developing an electrochemical method that transforms Pt nanospheres into shaped Pt NCs by using square-wave potential cycling [12]. Tetrahexahedral (THH) Pt nanoparticles enclosed by the {730}, {210}, {520} planes were prepared using this technique and showed high reactivity and stability. Moreover, trapezohedron enclosed by {522} facets [16], concave hexoctahedron by {321} and multiple twinned nanocrystals [17] were prepared by similar methods. However, from the practical applications point of view, it is still important to innovate synthesis technologies, which would enable to better control size, shape and yield as well as to involve different support substrates etc.

Herein we report a novel method for transformation of magnetron sputtered Pt thin films into Pt nanostructures enclosed by high-index facets, based on electrochemical square-wave potential cycling by using so-called twin working electrode (TWE) system. Contrary to previous works, based on transformation of structures as deposited on suitable substrate [12,17], our method allows to transform materials by transferring it from a one part (source) to another part (target) of the

* Corresponding author.
E-mail address: khalakhan@gmail.com (I. Khalakhan).

http://dx.doi.org/10.1016/j.surfcoat.2016.11.017
0257-8972/

working electrode in the form of nanostructures. This arrangement of the TWE system avoids the formation of any leftovers of untransformed Pt on the target part because it remains on the source part of TWE, which broadens horizons for future applications, e.g. deposition of nanostructures with high yield on different catalyst supports.

2. Materials and methods

2.1. Synthesis and materials

Electrochemical preparation of platinum nanostructures was carried out in a specially designed three-electrode electrochemical cell schematically shown in Fig. 1. It consists of a Pt ring wire counter electrode, a leak-free Ag/AgCl reference electrode (Innovative Instruments, Inc.) and a twin working electrode. The electrochemical cell was filled with 0.1 M H_2SO_4 solution prepared using deionized water (18.5 MΩ) and 95% pure H_2SO_4 acid (Sigma Aldrich).

A 50 nm platinum film sputter-deposited on a microporous carbon support (MCS, SGL TECHNOLOGIES GmbH, Sigratec GDL 25 BCE) (see Fig. S1) served as a source part of TWE in our setup. The deposition of Pt film was carried out using a DC operated magnetron from a 2 in. Pt target in Ar atmosphere with total pressure of 6×10^{-1} Pa.

A HOPG plate used as a substrate for deposition of nanostructures, served as the target part of the TWE. The trick is that the target part was mechanically attached to the source part, forming together TWE, as shown in Fig. 1. It should be noted that in this setup the TWE must be porous at least on one side in order to ensure the access of the electrolyte to the interface between the source and target parts.

The TWE system was then subjected to a series of oxidation/reduction square-wave potential cycles (3000 cycles) at frequency of 0.5 Hz using SP-150 Potentiostat (BioLogic Science Instruments).

2.2. Characterization techniques

Morphology of Pt nanostructures was examined by means of scanning electron microscopy (SEM) using a MIRA 3 Tescan microscope at 30 keV electron beam energy. Energy-dispersive X-ray spectroscopy (EDS) was done using a Bruker XFlash detector mounted directly into SEM. The crystallographic structure of Pt nanostructures was observed by transmission electron microscopy (TEM) using a 200 kV JEOL 2100F microscope with a Scherzer resolution of 0.19 nm.

3. Results and discussions

The electrochemical square-wave potential method has one unique characteristic – it involves periodic oxidation/reduction of platinum, which leads to the interplay between its dissolution and nucleation. During the oxidation part of cycling (E_U), the Pt film on the MCS substrate is oxidized and Pt atoms are partially dissolved in form of Pt^{2+} ions [12], filling the solution between electrodes. During the reduction part of cycling (E_L), the Pt^{2+} species are electroreduced to Pt atoms on both electrode parts, as the HOPG plate is in a direct contact with MCS, i.e. at the same potential. These two periodically repeated processes determine the growth of the platinum nanostructures on the HOPG substrate. An EDS spectrum in Fig. S2 confirms that Pt nanostructures, prepared in such way are composed of only Pt without any impurities.

The control of oxidation (E_U) and reduction (E_L) potentials is very important for a successful preparation of Pt nanostructures, using square-wave potential cycling [14,15,19,20]. Therefore, the set of experiments was carried out with the aim to investigate the potential dependence of Pt nanostructures formation. Cyclic voltammetry was used for determination of E_U and E_L in our setup in order to avoid oxygen and hydrogen evolution (see Fig. S3). It is important to note that all mentioned potentials are versus Ag/AgCl reference electrode. First, the synthesis of Pt nanostructures was implemented for various values of E_U, by keeping U_L constant at −0.3 V.

Fig. 2 illustrates a set of SEM images of Pt nanostructures, showing an evolution of the morphology and surface coverage with increasing E_U. Randomly oriented cubes with the size of about 70 nm were formed on the HOPG surface at $E_U = 1.0$ V (sample A). With increasing E_U to 1.1 V, we observed variously shaped particles about 100 nm in size (sample B). Some of these particles have the shape somehow similar to the THH Pt NCs, reported earlier [12], although our particles exhibit more defects. As E_U becomes more positive, i.e. 1.2 and 1.3 V, the products consist of mixed nanostructures with larger size, containing irregular nanoparticles and small nanorods (samples C and D, respectively). At 1.4 V, the formation of nanorods becomes more pronounced (sample E). In this case the length of nanorods is about 250 nm and the average diameter is about 100 nm.

The most important information is that except for differences in shape of the nanostructures, an increase of E_U leads to increasing amount of deposited Pt, i.e. to higher Pt coverages. This is evident from the SEM images taken at lower magnification (see upper images in Fig. 2). It means that higher oxidation potentials induce higher

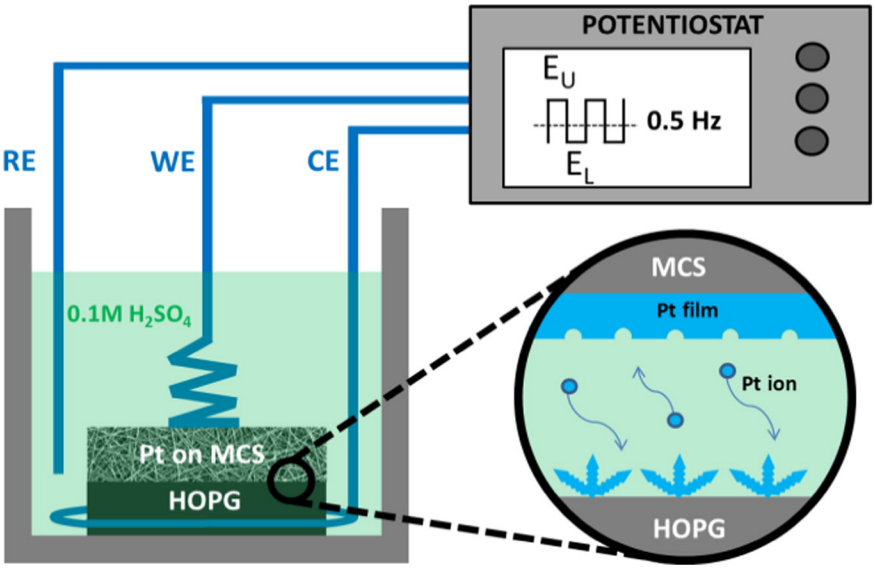

Fig. 1. Schematic illustration of twin working electrode (TWE) deposition system.

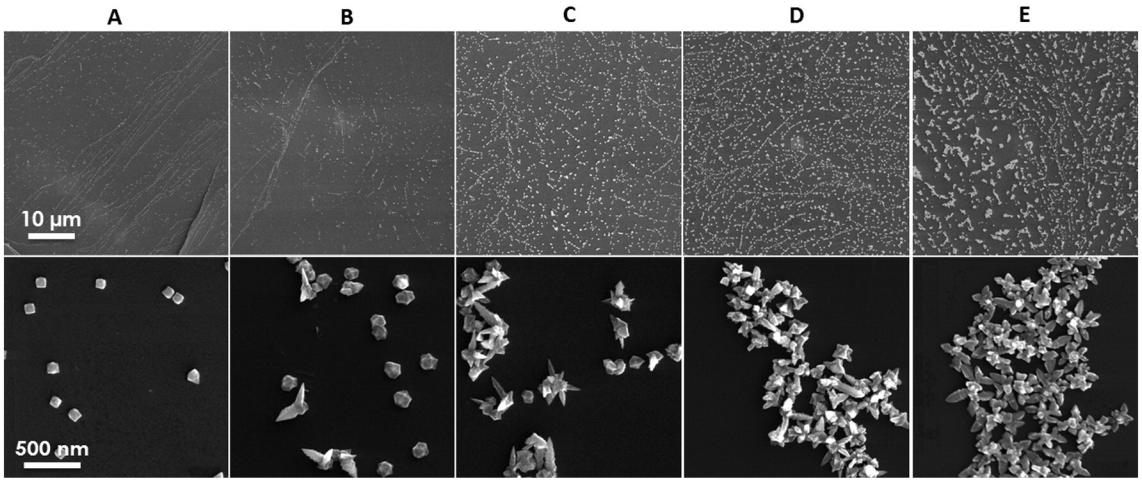

Fig. 2. SEM images of platinum nanostructures electrochemically prepared by square wave potential cycling at fixed $E_L = -0.3$ V as a function of oxidation potential: (A) $E_U = 1.0$ V; (B) $E_U = 1.1$ V; (C) $E_U = 1.2$ V; (D) $E_U = 1.3$ V; (E) $E_U = 1.4$ V. The view field of upper and bottom images is 50 μm and 2 μm, respectively.

amount of platinum to dissolve into the solution, and subsequently higher mass transport, which is in agreement with other data in the literature [18]. Higher coverage of Pt nanostructures was observed for samples D and E. For that reason, 1.4 V was chosen as fixed E_U for subsequent investigation of the influence of E_L on the morphology of Pt nanostructures.

Fig. 3 represents the SEM images of Pt nanostructures generated at different E_L and fixed E_U (1.4 V), under the same experimental conditions as in the previous experiment. At $E_L = -0.2$ V the formation of Pt nanorods with the length of about 500 nm and the average diameter of about 100 nm was observed (sample F). The structure of the nanorods looks similar to fivefold twinned Pt nanorods enclosed by high-index facets, prepared from Pt nanospheres using square-wave potential cycling [17]. Interestingly, the yield of these Pt nanorods was about 30% and the rest of platinum formed irregular nanostructures grown from residual parts of Pt nanospheres. In our case, due to the special twin electrode setup, the yield of Pt nanorods is substantially higher and they are not mixed with any residual Pt structures on the target HOPG substrate. Upon further increase of E_L to −0.1 V, nanorods become thinner (50 nm in diameter) and shorter (250 nm in length) (sample G in Fig. 3). Interestingly, the dendritic nanostructures were formed exclusively at $E_L = 0$ V (sample H). When E_L exceeds 0 V, neither nanorods nor Pt dendritic structures were produced; instead, the products consisted of mixed irregular Pt particles of very small coverage (samples I and J) [21]. However, a few imperfect dendritic nanostructures were still observed at $E_L = 0.1$ V (sample I).

A thorough inspection of all above presented samples proved that morphology of Pt nanostructures, electrochemically prepared in the TWE system is highly dependent on E_U and E_L potentials. By tuning the dynamic interplay between Pt dissolution process at E_U and platinum redeposition at E_L, we are able to tailor particle shape and coverages and thus controllably produce Pt nanostructures.

The sample H was chosen as the most interesting one for further characterization as dendritic structures possess high surface area, sharp edges and homogeneous shape distribution, which predetermine them for application in catalysis. In Fig. 4 high resolution (HR) SEM and HRTEM images of the sample H are plotted. Fig. 4a shows a SEM image of a platinum nanodendrites assembly, indicating that dendrites grow to different directions from one nucleation core, apparently formed at the early stage of the growth. From magnified SEM image in Fig. 4b it is clearly seen that each dendrite consists of one trunk and series of branches, which are parallel to each other and situated in the same plane as the trunk. The HRTEM image, taken from the area labelled c in Fig. 4b, shows the crystallographic structure of the tip of one

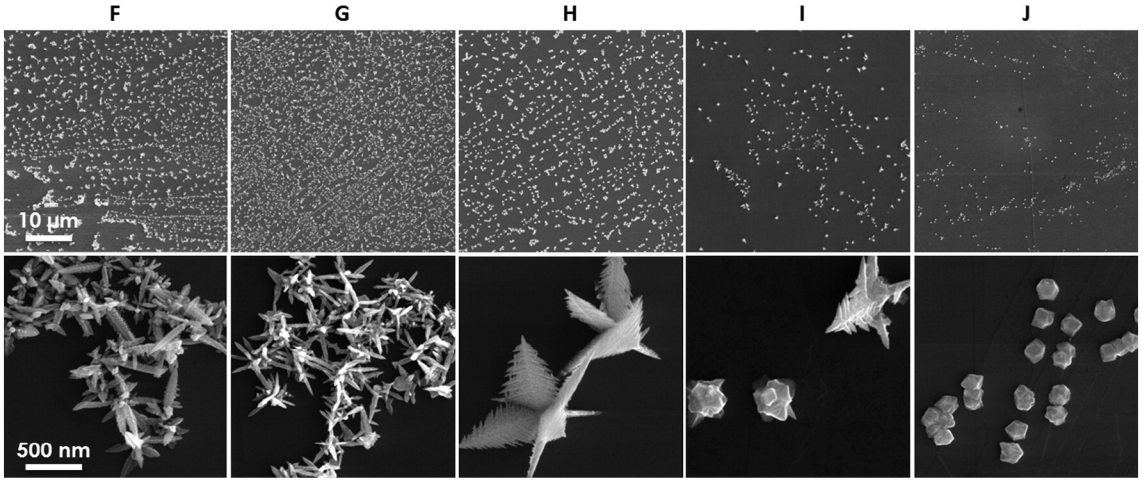

Fig. 3. SEM images of platinum nanostructures electrochemically prepared by square wave potential cycling at fixed $E_U = 1.4$ V as a function of reduction potential: (F) $E_L = -0.2$ V; (G) $E_L = -0.1$ V; (H) $E_L = 0$ V; (I) $E_L = +0.1$ V; (J) $E_L = +0.2$ V. The view field of upper and bottom images is 50 μm and 2 μm, respectively.

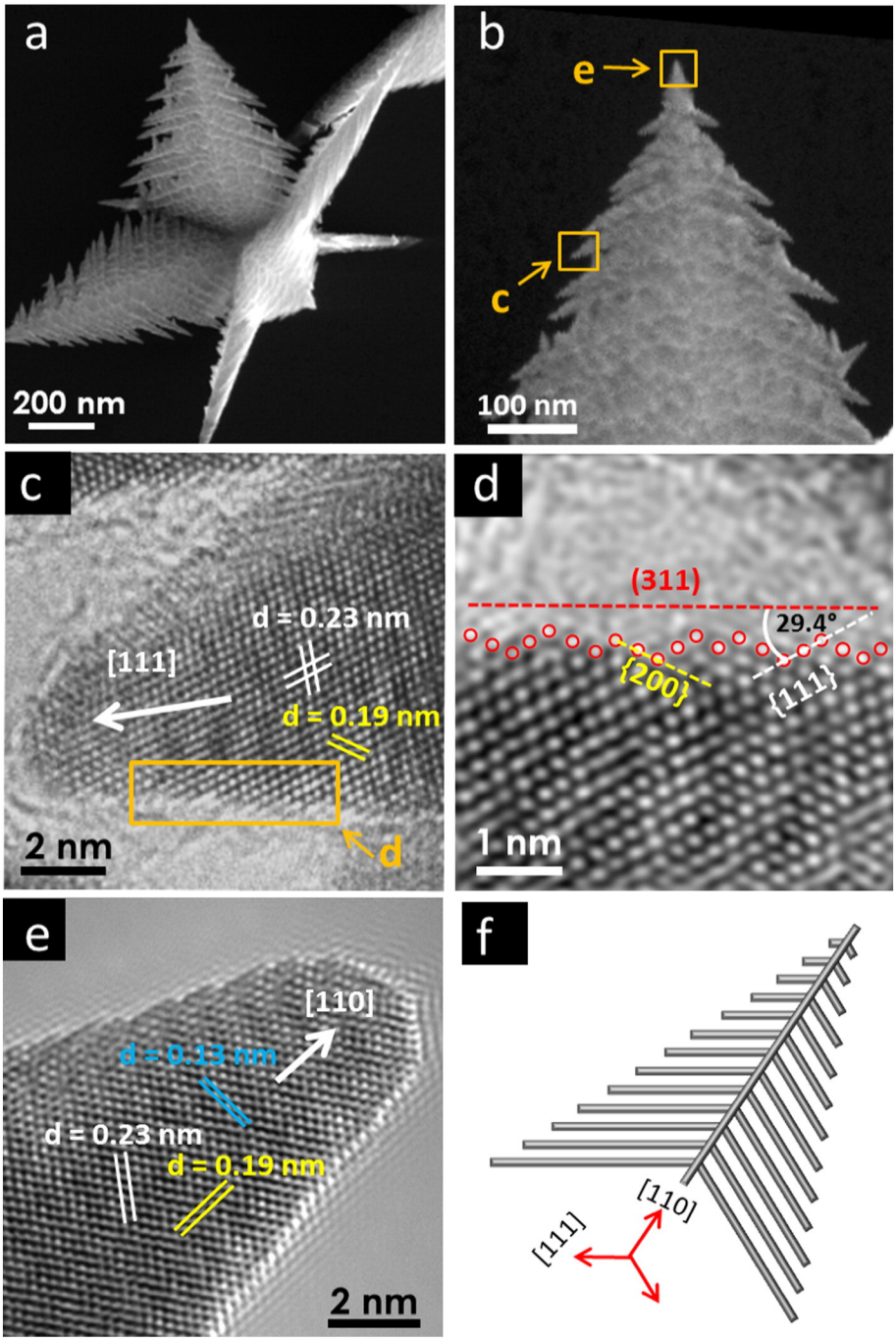

Fig. 4. High resolution SEM and HRTEM images of the sample H.

individual branch of the dendritic nanostructure (Fig. 4c). It clearly reveals a well ordered crystalline structure. The measured angles and lattice spacing of 0.23 nm, marked by white lines, and 0.19 nm, marked by yellow lines, correspond to the distances between the Pt {111} and {200} planes, respectively. The HRTEM image, thus, clearly indicates that the branch of the dendritic nanostructure grows in the [111] direction.

The HRTEM image of the highlighted region in Fig. 4c presented in Fig. 4d shows a lattice structure of the edge of dendrite branch. An interfacial angle of 29.4° measured between the edge facet and the {111} plane is in good agreement with a theoretical value of 29.4° corresponding to the angle between {311} and {111} facets. The atomic arrangement of the Pt (311) surface is periodically composed of the (200) and (111) terraces, forming a stepped structure [22] which is consistent with the atomic arrangement of the edge steps, shown in Fig. 4d. Fig. 4e, in turn, shows HRTEM image taken from the area labelled e in Fig. 4b i.e. the tip of the dendrite trunk. The growth direction was measured to be [110]. Based on above results, we can determine two preferential growth directions in case of the sample H: the growth direction of the nanostructures trunk is [110], while the growth of its individual branches is along the [111] direction (see model in Fig. 4f).

It is well known that the nucleation process determines the growth of shaped metal nanostructures. In order to gain a clear picture of Pt nanostructures growth, we followed the growth of the sample H from the very first steps. In addition to the sample H, we provided the same experiment on the sample G, in order to understand formation process of nanostructures with different shapes. We prepared series of intermediate nanostructures by controlling the deposition time i.e. the number

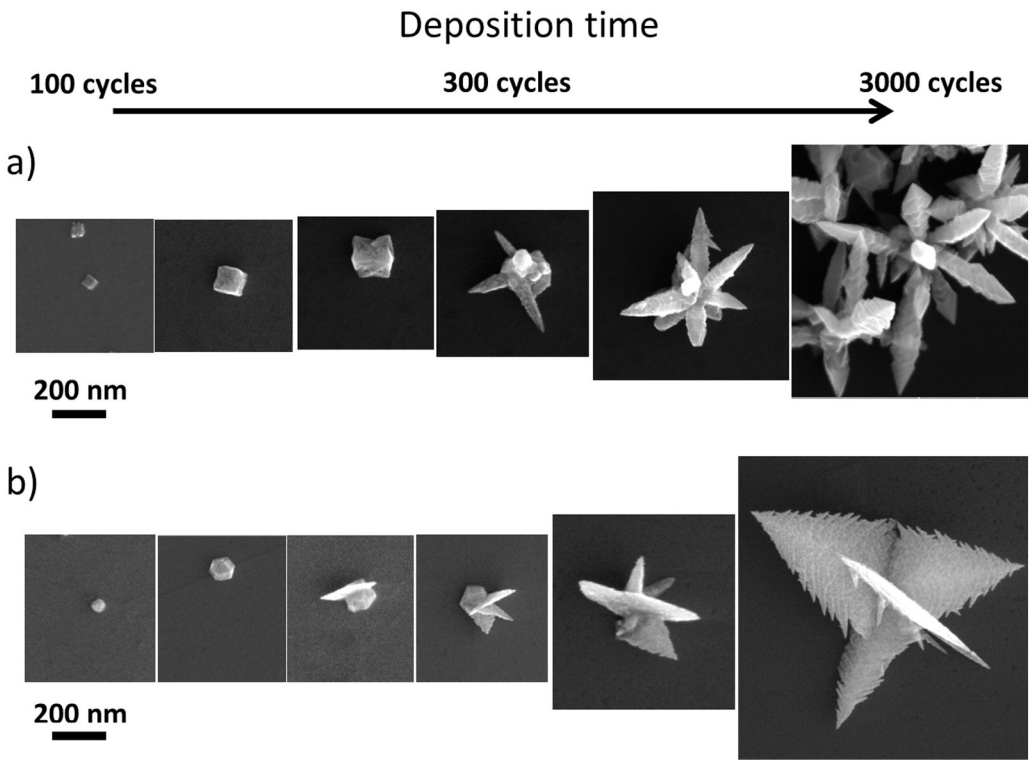

Fig. 5. Shape evolution of Pt nanostructures as a function of deposition time (number of cycles): a) sample G and b) sample H.

of oxidation/reduction square-wave potential cycles (from 100 to 3000). Fig. 5a shows the shape evolution of the sample G during square potential cycling, measured by SEM.

At the very beginning of the growth (100 cycles) small cubic nanoparticles are formed (for better detail see Fig. S4). Upon increasing number of cycles, we observed morphological transformation of the small cubes to concave cubes of larger sizes. An overgrowth of Pt nanocube nuclei along their corners and ridges, i.e. along [111] and [110] directions, respectively, is occurring due to faster growth of sharp edges, capturing a larger amount of Pt ions from solution [23]. The further NPs growth is determined by these directions. In case of the sample H, the shape of nanocrystals formed during nucleation phase is completely different (Fig. 5b). At the early stage of the growth (100 cycles) small nanoparticles are formed and then transformed to rhombic dodecahedron (RD) nanocrystals with increasing number of cycles (for better detail see Fig. S5). Indeed, it can be seen from Fig. 5b that the dendritic nanostructures growth is determined by RD because they start to grow directly from the RD ridges.

At the beginning of the nanostructure growth, Pt ions formed on the source electrode are electro-reduced and nucleate on the HOPG substrate at each oxidation/reduction cycle, forming Pt nanoparticles. These nanoparticles become the seeds for further growth of nanostructures. In Fig. 5 it can be seen that the shape of the nanocrystals varies with applied reduction potential from a cube, for the sample G ($E_L = -0.1$ V, $E_U = 1.4$ V), to a rhombic dodecahedron, for the sample H ($E_L = 0$ V, $E_U = 1.4$ V). Such evolution of the NCs shape induced by different E_L and E_U during square-wave potential cycling was explained through the simultaneously acting place-exchange mechanism between platinum and oxygen atoms, oxidative etching at E_U and growth rate at E_L [19]. Further increase of the potential cycling time would lead to overgrowth of shaped nanocrystals. Since the pulse frequency used in our experiment is relatively low (0.5 Hz), the observed overgrowth can be explained in terms of classical theory of the electrodeposition from an electrolyte at each cycle [15]. According to the theory, higher concentration of deposited metal ions is formed in the electrolyte near the sharp parts of nanocrystals than near their flat parts, due to the effect of so-called spherical diffusion layers [24–26], which results in heterogeneity of the growth. Indeed, upon further increasing of deposition time, we observed preferential growth of sharp features (Fig. 5). In case of the sample H, however, we observed more than one growth directions, which led to the formation of dendrite-like nanostructures. Dendritic growth is the part of the theory of electrodeposition, when during the growth protrusions occur [25,26] which act as a source for the formation of secondary spherical diffusion layers and thus would overgrow simultaneously with the growth of the main stem, causing the formation of branched nanostructures. Generally, dendrite formation depends on many factors such as a concentration of ions in the solution [26,27], applied potential [15,28,29], stabilization agents [30,31], potential cycling frequency [32] etc. Since in our setup we do not have any stabilization agents and cycling frequency was equal for all samples, we can conclude that the reduction potential E_L plays the key role in the formation of different Pt nanostructures. If E_L is more positive (note that more positive potential is equivalent to lower overpotential in cathodic deposition), nucleation rate is lower, which leads to Pt atoms more likely to migrate from regions with high surface energy to regions with lower surface energy, forming therefore thermodynamically more favorable shapes. This explains formation of irregular nanocrystals in the case of sample J and I, where the lowest overpotential values were applied (Fig. 3). As the E_L decreases towards more negative values, the reduction rate becomes higher and limits surface diffusion, which leads to only sharp parts overgrowth. However, some protrusions are still formed, thus facilitating Pt dendrites formation in case of the sample H. Further increase of overpotential would limit the diffusion even more, causing ions deposition only on sharp parts, where the electric field is higher, resulting in nanorod-shape growth as observed in case of samples G and F (Fig. 3). At the same time, the unique characteristic of the electrochemical square-wave potential cycling would result in the formation of high-index facets. In literature it has been reported that low-index facets are unstable in square-wave potential conditions and could be deconstructed by periodic adsorption and desorption of

oxygen, forming more stable high-index facets [12,19,33]. Likewise, the observation of the {311} facets of the dendritic branches in our experiment is in accordance with the abovementioned mechanism.

4. Conclusions

In this work we have presented specially designed twin working electrode (TWE) system which allows transforming Pt thin films into various three-dimensional Pt nanostructures by means of square-wave potential cycling. It was shown that by tuning the dynamic interplay between oxidation and reduction potentials it is possible to tailor nanostructures shapes and coverages. Moreover, the nanostructures were found to be enclosed by thermodynamically unfavorable high-index facets, which mean that high densities of atomic steps, edges, and kinks are exposed on their surfaces. The described controllable formation of nanostructures indicates that the proposed method can be applied to achieve the selective growth of high purity Pt nanostructures with specific shapes (facets or edges).

Usage of magnetron sputtering for preparation of the source electrode is of particular interest because it can be used to homogeneously coat large areas with any material. Together with the simple TWE configuration it makes the setup potentially suitable for production of nanostructures supported on larger carbon substrates. Moreover, this inexpensive and relatively fast route can be extended to synthesize nanostructures of other noble materials as well as usage of different supports, which makes the described method a versatile way to create electrodes for various applications in the fields of catalysis.

Acknowledgments

The authors acknowledge financial support by the EU (FP7 NMP Project ChipCAT No. 310191, the Central European Research Infrastructure Consortium (CERIC) project), the Czech Science Foundation (grant 13-10396S) and Romanian Ministry of Education (through the Core Program, Project PN16-480102). J. Lavková acknowledges the Charles University Grant Agency (GAUK 358615) for research support.

Appendix A. Supplementary data

Supplementary data to this article can be found online at http://dx.doi.org/10.1016/j.surfcoat.2016.11.017.

References

[1] S. Guo, E. Wang, Noble metal nanomaterials: controllable synthesis and application in fuel cells and analytical sensors, Nano Today 6 (2011) 240–264.
[2] H. Zhang, M. Jin, Y. Xia, Noble-metal nanocrystals with concave surfaces: synthesis and applications, Angew. Chem. Int. Ed. 51 (2012) 7656–7673.
[3] W. Niu, G. Xu, Crystallographic control of noble metal nanocrystals, Nano Today 6 (2011) 265–285.
[4] A.R. Tao, S. Habas, P. Yang, Shape control of colloidal metal nanocrystals, Small 4 (2008) 310–325.
[5] V. Komanicky, H. Iddir, K.C. Chang, A. Menzel, G. Karapetrov, D. Hennessy, P. Zapol, H. You, Shape-dependent activity of platinum array catalyst, J. Am. Chem. Soc. 131 (2009) 5732–5733.
[6] E. Schmidt, A. Vargas, T. Mallat, A. Baiker, Shape-selective enantioselective hydrogenation on Pt nanoparticles, J. Am. Chem. Soc. 131 (2009) 12358–12367.
[7] B. Zhang, D. Wang, Y. Hou, S. Yang, X.H. Yang, J.H. Zhong, J. Liu, H.F. Wang, P. Hu, H.J. Zhao, H.G. Yang, Facet-dependent catalytic activity of platinum nanocrystals for triiodide reduction in dye-sensitized solar cells, Sci. Rep. 3 (2013) 1836–1842.
[8] K. An, G.A. Somorjai, Size and shape control of metal nanoparticles for reaction selectivity in catalysis, ChemCatChem 4 (2012) 1512–1524.
[9] S. Xie, S.I. Choi, X. Xia, Y. Xia, Catalysis on faceted noble-metal nanocrystals: both shape and size matter, Curr. Opin. Chem. Eng. 2 (2013) 142–150.
[10] G.A. Somorjai, D.W. Blakely, Mechanism of catalysis of hydrocarbon reactions by platinum surfaces, Nature 258 (1975) 580–583.
[11] S.G. Sun, A.C. Chen, T.S. Huang, J.B. Li, Z.W. Tian, Electrocatalytic properties of Pt(111), Pt(332), Pt(331) and Pt(110) single crystal electrodes towards ethylene glycol oxidation in sulphuric acid solutions, J. Electroanal. Chem. 340 (1992) 213–226.
[12] N. Tian, Z.Y. Zhou, S.G. Sun, Y. Ding, Z.L. Wang, Synthesis of tetrahexahedral platinum nanocrystals with high-index facets and high electro-oxidation activity, Science 316 (2007) 732–735.
[13] L. Zhang, W. Niu, G. Xu, Synthesis and applications of noble metal nanocrystals with high-energy facets, Nano Today 7 (2012) 586–605.
[14] L. Wei, Z.Y. Zhou, S.P. Chen, C.D. Xu, D. Su, M.E. Schuster, S.G. Sun, Electrochemically shape-controlled synthesis in deep eutectic solvents: triambic icosahedral platinum nanocrystals with high-index facets and their enhanced catalytic activity, Chem. Commun. 49 (2013) 11152–11154.
[15] J. Liu, X. Wang, Z. Lin, Y. Cao, Z.Z. Zheng, Z. Zeng, Z. Hu, Shape-controllable pulse electrodeposition of ultrafine platinum nanodendrites for methanol catalytic combustion and the investigation of their local electric field intensification by electrostatic force microscope and finite element method, Electrochim. Acta 136 (2014) 66–74.
[16] Y. Li, Y. Jiang, M. Chen, H. Liao, R. Huang, Z. Zhou, N. Tian, S. Chen, S. Sun, Electrochemically shape-controlled synthesis of trapezohedral platinum nanocrystals with high electrocatalytic activity, Chem. Commun. 48 (2012) 9531–9533.
[17] Z.Y. Zhou, N. Tian, Z.Z. Huang, D.J. Chen, S.G. Sun, Nanoparticle catalysts with high energy surfaces and enhanced activity synthesized by electrochemical method, Faraday Discuss. 140 (2008) 81–92.
[18] D.F. Untereker, S. Bruckenstein, A dissolution-redeposition mechanism for the roughening of platinum electrodes by cyclic potential programs, J. Electrochem. Soc. 121 (1974) 360–362.
[19] J. Xiao, S. Liu, N. Tian, Z.Y. Zhou, H.X. Liu, B.B. Xu, S.G. Sun, Synthesis of convex hexoctahedral Pt micro/nanocrystals with high-index facets and electrochemistry-mediated shape evolution, J. Am. Chem. Soc. 135 (2013) 18754–18757.
[20] N. Tian, Z.Y. Zhou, S.G. Sun, L. Cui, B. Ren, Z.Q. Tian, Electrochemical preparation of platinum nanothorn assemblies with high surface enhanced Raman scattering activity, Chem. Commun. 39 (2006) 4090–4092.
[21] K.H. Kim, J.Y. Zheng, W. Shin, Y.S. Kang, Preparation of dendritic NiFe films by electrodeposition for oxygen evolution, RSC Adv. 2 (2012) 4759–4767.
[22] L. Yang, X. Song, M. Qi, L. Xia, M. Jin, Templated high-yield synthesis of Pt nanorods enclosed by high-index {311} facets for methanol selective oxidation, J. Mater. Chem. A 1 (2013) 7316–7320.
[23] N. Tian, Z.Y. Zhou, S.G. Sun, Platinum metal catalysts of high-index surfaces: from single-crystal planes to electrochemically shape-controlled nanoparticles, J. Phys. Chem. C 112 (2008) 19801–19817.
[24] C.D. Owen, M.G. Norton, Growth mechanism of one dimensional tin nanostructures by electrodeposition, J. Mater. Sci. 51 (2016) 577–588.
[25] M.I. Čekerevac, K.I. Popov, Dendritic electrocrystallization of cadmium from acid sulphate solution III: the effect of overpotential, Surf. Coat. Technol. 37 (1989) 441–447.
[26] J.L. Barton, J.O.M. Bockris, The electrolytic growth of dendrites from ionic solutions, Proc. R. Soc. Lond. A 268 (1962) 485–505.
[27] J. Fang, H. You, P. Kong, Y. Yi, X. Song, B. Ding, Dendritic slver nanostructure growth and evolution in replacement reaction, Cryst. Growth Des. 7 (2007) 864–867.
[28] E.R. White, S.B. Singer, V. Augustyn, W.A. Hubbard, M. Mecklenburg, B. Dunn, B.C. Regan, In situ transmission electron microscopy of lead dendrites and lead ions in aqueous solution, ACS Nano 6 (2012) 6308–6317.
[29] Y.J. Song, J.Y. Kim, K.W. Park, Synthesis of Pd dendritic nanowires by electrochemical deposition, Cryst. Growth Des. 9 (2009) 505–507.
[30] Y. Ni, Y. Zhang, J. Hong, Potentiostatic electrodeposition route for quick synthesis of featherlike PbTe dendrites: influencing factors and shape evolution, Cryst. Growth Des. 11 (2011) 2142–2148.
[31] J. Xiao, L. Qi, Surfactant-assisted, shape-controlled synthesis of gold nanocrystals, Nanoscale 3 (2011) 1383–1396.
[32] L. Zeiri, S. Efrima, M. Deutsch, AC-driven interfacial electrodeposition of silver, Langmuir 13 (1997) 4722–4728.
[33] N. Furuya, M. Shibata, Structural changes at various Pt single crystal surfaces with potential cycles in acidic and alkaline solutions, J. Electroanal. Chem. 467 (1999) 85–91.